JGR Biogeosciences

RESEARCH ARTICLE
10.1029/2019JG005604

Sources, Transformation, and Fate of Dissolved Organic Matter in the Gravel Bar of a Prealpine Stream

Kyle S. Boodoo[1,2], **Christina Fasching**[3], **and Tom J. Battin**[4]

[1]Department of Limnology and Bio-Oceanography, University of Vienna, Austria, [2]EcoCatch, WasserCluster Lunz—Biological Station GmbH, Lunz am See, Austria, [3]Department of Soil Ecology, Helmholtz Centre for Environmental Research—UFZ, Halle, Germany, [4]Stream Biofilm and Ecosystem Research Laboratory, ENAC, Ecole Polytechnique Fédérale de Lausanne, Lausanne, Switzerland

Abstract Gravel bars (GBs) are hotspots of biogeochemical activity, likely impacting carbon dynamics in streams and rivers. However, it remains unclear how GBs process dissolved organic matter (DOM) received from stream water and groundwater. Here we investigate the spatial and temporal variability of DOM concentration and composition within a GB using DOM absorbance and fluorescence measurements. We found clear seasonal and diurnal patterns in DOM composition within the GB, indicating changing contributions of DOM sources and transformation processes. While DOM composition was characterized by more protein-like DOM in summer, with increasing contributions of humic-like DOM toward winter within the stream water and GB, groundwater DOM exhibited a strong aromatic and humic-like character year-round. DOM composition and concentration varied diurnally during autumn and winter within the GB and stream water, while seasonally higher groundwater inputs in summer likely muted the diurnal pattern, pointing to the importance of seasonal hydrological controls on DOM dynamics. Mixing model analysis showed GB DOM characteristics to differ from that predicted by stream water-groundwater mixing within the GB, particularly in summer. Dissolved organic carbon concentration decreased along flow paths through the GB with increasing residence time, likely pointing to microbial uptake and/or adsorption to sediment surfaces within the GB, with concurrent clear shifts in DOM composition. While freshly produced and more humified DOM increased along GB flow paths, protein-like fluorescence (C3) was removed, indicating the simultaneous production and removal of DOM. Together, our findings highlight the role of GBs in DOM removal and transformation, influenced by seasonal shifts in temperature and hydrodynamics.

Plain Language Summary Gravel bars (GBs) are common raised in-stream structures which promote stream water flow into the streambed and mixing with groundwater. Such mixing zones have been shown to be hotspots of biogeochemical activity. Here we investigate how GBs change organic matter received by stream water and groundwater. Overall, we found that organic matter was both transformed and removed from the GB, likely as a result of microbial activity and/or attachment of organic matter to GB sediment surfaces. Slower flow of water through the GB during lower discharges resulted in higher rates of organic matter change and removal. Further analysis showed simultaneous production of fresh organic matter and removal of source organic matter within the GB. Together, our findings highlight the role of seasonal shifts in temperature and stream water-groundwater mixing in these processes.

Key Points:
- Gravel bar dissolved organic matter concentration and composition significantly differs from that predicted by the mixing of its end-members
- Dissolved organic matter composition within both the stream and gravel bar generally differed across seasonal and diurnal timescales
- Longer exposure times and warmer temperatures increase alteration of gravel bar dissolved organic matter concentration and composition

Supporting Information:
- Supporting Information S1

Correspondence to:
K. S. Boodoo, kyle.boodoo@univie.ac.at

Citation:
Boodoo, K. S., Fasching, C., & Battin, T. J. (2020). Sources, transformation, and fate of dissolved organic matter in the gravel bar of a prealpine stream. *Journal of Geophysical Research: Biogeosciences*, *125*, e2019JG005604. https://doi.org/10.1029/2019JG005604

Received 12 DEC 2019
Accepted 4 JUN 2020
Accepted article online 2 JUL 2020

Author Contributions:
Conceptualization: Kyle S. Boodoo, Tom J. Battin
Data curation: Kyle S. Boodoo
Formal analysis: Kyle S. Boodoo
Funding acquisition: Tom J. Battin
Investigation: Kyle S. Boodoo
Methodology: Kyle S. Boodoo, Christina Fasching, Tom J. Battin
Project administration: Tom J. Battin
Resources: Tom J. Battin
Software: Kyle S. Boodoo
Supervision: Tom J. Battin
Validation: Kyle S. Boodoo, Christina Fasching
(continued)

1. Introduction

Inland waters, including streams and rivers, represent a significant and active component of the global carbon cycle and are recipient to a substantial amount of dissolved organic matter (DOM) from their surrounding terrestrial environment via lateral fluxes, as well as in situ production by algae, submerged vegetation, and biofilms (Battin et al., 2009; Hotchkiss et al., 2015; Raymond et al., 2013; Raymond & Spencer, 2015). Along the stream corridor, DOM can be transformed and respired by aquatic heterotrophs within the stream and bed sediments, contributing to CO_2 fluxes from stream ecosystems (Guillemette & Giorgio, 2012), or altered by physical processes, including photodegradation (Kragh et al., 2008; Tranvik & Bertilsson, 2001). Additionally, DOM can be removed via the adsorption of dissolved organic carbon (DOC) onto sediment surfaces or incorporation within attached biofilms in stream corridor sediments (Battin et al., 2008; Findlay & Sobczak, 1996; Hunter et al., 2016), transiently retaining DOM over a range of seasonal and hydrological conditions as has been shown to occur in gravel bar (GB) sediments (Findlay & Sobczak, 1996). In fact,

Visualization: Kyle S. Boodoo
Writing - original draft: Kyle S. Boodoo, Christina Fasching, Tom J. Battin
Writing – review & editing: Kyle S. Boodoo, Christina Fasching

GBs have been recognized as sites of increased DOC removal (Findlay et al., 1993; Findlay & Sobczak, 1996) and DOM processing (Vervier et al., 1993) and, more recently, as hotspots of CO_2 evasion within stream corridors (Boodoo et al., 2017). These common in-stream structures were shown to evade more than double the amount of CO_2 than the surrounding stream water (SW), with a large percentage of the CO_2 potentially originating from aerobic heterotrophic respiration (Boodoo et al., 2019). Furthermore, CO_2 derived from soil respiration and physical weathering of calcareous rock may be delivered to the stream via groundwater (GW) upwelling, representing a significant source of CO_2 to the stream, modulated by site-specific hydrological characteristics and event-driven hydrodynamics (Duvert et al., 2018; Horgby et al., 2019; Hotchkiss et al., 2015). Yet, how GBs process the received DOM from different sources within the stream corridor, leading to CO_2 outgassing, remains not well understood.

Terrestrial inputs of DOM to the stream can be diverse, including soil carbon delivered by shallow or deeper GW, direct leaf litter, and riparian soil surface layer inputs during overland flow, leaf fall, and aerial deposition of sediment (Inamdar et al., 2011; Singh et al., 2014). While this DOM is often considered comparatively more refractory to microbial metabolism (Schmidt et al., 2011), other studies have shown that GW can be a source of bioavailable DOM, nutrients, and bacterial community heterogeneity within streams and the hyporheic zone (Boissier et al., 1996). However, in situ production of DOM by benthic algae and microbial activity within the SW column, streambed surface, and hyporheic zone can represent an important source of more labile autochthonous DOM (Kaplan & Bott, 1989) within the stream and hyporheic sediments. As the reactivity and bioavailability of these different DOM components may differ substantially (Cory & Kaplan, 2012), the overall reactivity of the DOM pool within the stream and its hyporheic zone is likely dependent on the magnitude of the different DOM source contributions.

The fate of DOM within GBs and the stream corridor, whether it is transformed or transported downstream largely unchanged, is determined not only by its chemical composition but also the stream channel morphology and prevailing hydrodynamic conditions. Topographical variability in the streambed, such as small bedforms, GBs, and larger riffle-pool sequences, induce hydrodynamically driven exchange of water between the stream and its subsurface, resulting in the mixing of SW and GW within the hyporheic zone (Stonedahl et al., 2010; Tonina & Buffington, 2007) and their distinct DOM pools. Meanwhile, residence time, determined by hydrodynamic and sediment characteristics within the stream corridor, acts as a major constraint of physical and biological processes linked to DOM alteration and removal within aquatic systems (Battin et al., 2008; Casas-Ruiz et al., 2017), such as photooxidation (Kragh et al., 2008; Tranvik & Bertilsson, 2001) and microbial respiration and production of autochthonous DOM (Guillemette & Giorgio, 2012). Furthermore, temperature and nutrient availability (Berggren et al., 2010; Casas-Ruiz et al., 2017; Yvon-Durocher et al., 2012), as well as microbial community composition (Battin et al., 2008), act as physical and biological controls on microbial respiration and DOM alteration within stream corridors.

GBs induce SW downwelling (Boodoo et al., 2019; Hester & Doyle, 2008; Tonina & Buffington, 2009), promoting the mixing of SW and GW below the GB, locally extending the hyporheic zone. The hyporheic zone is a site of increased biogeochemical cycling and heterotrophic metabolism (Mulholland et al., 1997), DOC production (Schindler & Krabbenhoft, 1998), and nitrification (Dahm et al., 1998). This high biogeochemical reactivity has been attributed to relatively high oxygen and nutrient inputs to the hyporheic zone, typically originating from SW and GW hyporheic end-members, respectively (Bardini et al., 2012; Boano et al., 2014; Boulton et al., 2010; Harvey & Fuller, 1998). Additionally, longer residence times within the hyporheic zone than the stream itself facilitate an increased opportunity for biogeochemical transformations (Findlay, 1995; Kasahara & Wondzell, 2003), while more stable temperatures, which may be higher than the stream mean diurnal and seasonal temperature, due to lagged stream water temperature effects (Arrigoni et al., 2008), further provide conditions favorable for biogeochemical reactions.

The degree to which SW and GW mix within GBs depends on hydraulic head differences between the SW and GW, the amplitude of the streambed structure and thickness (Boano et al., 2014; Tonina & Buffington, 2011; Trauth et al., 2014; Wu et al., 2018). Mixing of SW and GW within the GB subsurface likely leads to a unique mixture of DOM—an aggregate of DOM ranging from highly labile to more recalcitrant, and simple low molecular weight molecules to more complex DOM. Exposure of this unique mixture of DOM to prevailing physicochemical conditions within the GB, such as more stable temperatures, elevated oxygen concentrations, and longer residence times, may favor increased rates of DOM alteration via

microbial degradation and heterotrophic metabolism. GBs can absorb, store, and transfer heat in warmer months from its surface downward into the GB hyporheic zone below, likely enhancing the rate of microbial activity and other processes therein (Boodoo et al., 2017). Thus, GBs can potentially play an important role in the transformation of SW and GW DOM on the reach scale by increasing hyporheic flow within streams.

Here we investigate the variability in DOC concentration and DOM composition within a prealpine GB, as well as the stream and shallow GW, over diurnal to seasonal timescales to determine the role of GBs in stream carbon cycling. Using hydrological data from a previous study, we identify major SW downwelling flow paths and follow the change in DOM composition along the flow paths through the GB during different seasonal discharges. We investigate the role of stream discharge, residence time, and seasonal temperatures, as well as the apparent degree of SW-GW mixing on DOM composition and transformation. Overall, we highlight GBs as sites of significant DOM transformation and removal within stream corridors, with the degree of transformation dependent on stream hydrodynamics and seasonal changes in temperature.

2. Materials and Methods

2.1. Sampling Site Description

We investigated variability in DOC concentration and composition within a point GB and associated stream corridor of the Oberer Seebach (OSB) (Figures 1a, 1d, and 1e). OSB is a third-order stream (47°51′08″N, 15°03′54″E, 600 m above sea level) which drains a largely pristine catchment (20 km^2) in the eastern Alps (Lunz am See, Austria). The stream sediment and GB are characterized by a calcareous armor layer overlaying glacial alluvial deposits and ancient lake sediment; sediment porosity is relatively high (29%), and stream slope is 0.41% (Battin, 1999). At the annual average discharge (0.75 $m^3\ s^{-1}$, 2010–2016), the GB exposed surface measures ~29 m in length and 4.5 m in width. The OSB hydrograph is characterized by multiple snowmelt peaks in spring (up to 28.1 $m^3\ s^{-1}$) and extended baseflow periods (0.07 $m^3\ s^{-1}$) in summer. The studied section of the OSB is predominantly losing and receives shallow GW flow from the nearby riparian zone hillslope on the left bank side of the GB toward the opposite right bank floodplain (Boodoo et al., 2019). A distinct side channel (SC), predominantly fed by throughflow from the main channel, is located between the GB and its left bank (Figure 1a). The SC is characterized by the presence of several isolated pools at discharges above baseflow and becomes fully connected to the main stream at above annual mean discharges. The OSB SW is characterized as typically oxygen supersaturated (dissolved oxygen: 111 to 119%) and has a long-term average pH and electrical conductivity (EC) of 8.0 ± 0.2 and 232.4 ± 13.9 $\mu S\ cm^{-1}$, respectively (Boodoo et al., 2019). The surrounding riparian vegetation is dominated by *Fraxinus excelsior*, *Acer pseudoplatanus*, *Fagus sylvatica*, *Salix caprea*, and *Picea abies* (Battin, 1999).

2.2. Sampling Methodology

Monthly sampling of GB (eight locations) and SC (five locations) pore water, in addition to OSB SW and GW, was conducted between May 2015 and March 2016 in order to determine the sources and fate of DOM within the GB and SC (Figure 1a). For ease of comparison and to help better describe spatial variability, we separated GB and SC sampling locations into groups based on their location in relation to the OSB main channel (SW) and hillside riparian zone. The GB was separated into three sections, from the most upstream in the direction of streamflow: head, crest, and tail. The SC group represented the sampling locations within or closest to the temporary channel on the hillslope side of the GB (Figure 1a).

All porewater samples were extracted along two horizontal planes: GB_{up} and GB_{low} (610.31 ± 0.05 and 609.81 ± 0.05 m above sea level—corresponding to 0.75 and 1.25 m depth below GB surface, reference: highest point of GB crest surface), respectively. SW was sampled at midwater column depth, just upstream of the GB, while GW samples were extracted from a shallow riparian GW well on the left bank of the stream, where GW flow toward the stream had been previously identified (Battin, 1999). Sampling months were separated into seasonal groups (Summer: May–September; Autumn: October–November; and Winter: December–March), as discharge, temperature, and other climatic and environmental factors which typically vary with seasons may have affected DOM characteristics within the stream corridor.

In order to investigate diurnal variability of DOM over different seasons, we conducted three high-resolution diurnal samplings [5:00, 14:00, 20:00] over a total of 5 to 7 days each, in September 2015 (summer), November 2015 (autumn), and March 2016 (winter). High-resolution samplings were conducted at a

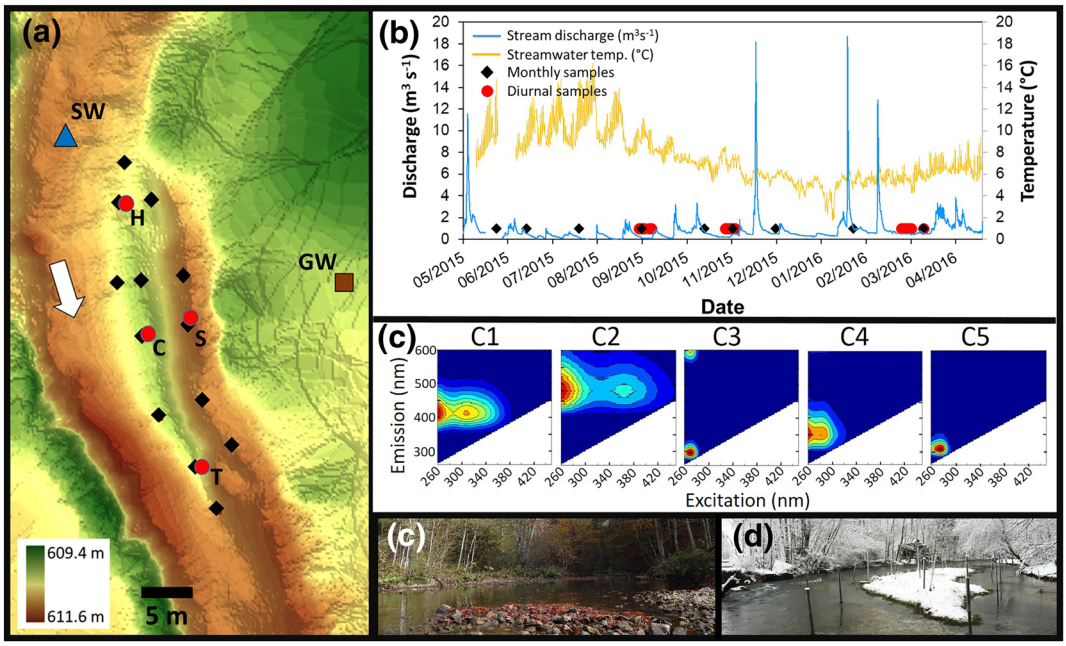

Figure 1. Composite figure showing the OSB sampling site: (a) Monthly sampling locations are depicted as black diamonds, seasonal sampling locations as red circles (H = head, C = crest, T = tail, S = side channel), and stream water (SW) and groundwater (GW) as a blue triangle and brown square, respectively. The GB head is connected to the left streambank, restricting surface flow along the side channel (SC) during low discharges. The white arrow shows the OSB stream water flow direction. (b) Time series showing OSB stream discharge ($m^3\ s^{-1}$), temperature (°C), and the timing of different sampling events. Monthly samples (sampling time ~ 9:00–15:00) were taken across 13 GB locations, while diurnal samples were taken at 5:00, 14:00, and 20:00 during 5–7 consecutive days. All GB samples were taken at two depths (GB_{up} and GB_{low}, corresponding to 0.75 and 1.25 m below GB crest), and corresponding OSB stream water and shallow riparian zone GW samples were taken during all samplings. (c) To investigate DOM composition variability, we conducted parallel factor analysis of all samples, identifying five individual DOM components (C1–C5). (d) Upstream view from GB showing entrainment of fallen leaves around GB during autumn and (e) restoration of SC flow with that of the main OSB channel during winter flow conditions.

single location within the GBs head, crest, tail, and SC sections, in addition to the SW and GW (Figure 1a). Average SW discharge and temperature during diurnal high-resolution sampling was 0.07 $m^3\ s^{-1}$, 10.2°C (Summer), 0.31 $m^3\ s^{-1}$, 7.5°C (Autumn), and 0.48 $m^3\ s^{-1}$, 5.4°C (Winter).

During each sampling event, we collected water samples for analysis of DOC, DOM absorbance, and fluorescence. Additionally, we measured in situ temperature, oxygen concentration, and EC of all samples. Hyporheic water samples were obtained at two depths from 13 piezometer pairs (PVC tubing, 6 mm inner diameter, wall thickness 2 mm) located at the GB head, crest, tail, and SC. All piezometers were located below the long-term GB low water table and samples slowly extracted via an electric pump (12V-N86KNDC, KNF Neuberger Inc, NJ, USA) and connected tubing into combusted (450°C, 5 hr), 250 ml Schott® bottles. In situ temperature and dissolved oxygen at all locations were measured using an oxygen dipping probe (TSUB21-CL5, PyroScience GmbH, Aachen, Germany). EC was measured following oxygen and temperature measurements and subsamples extracted for later DOC concentration measurements and DOM absorbance and fluorescence scans. The EC probe was rinsed with a small amount of the sample to be analyzed before the testing and recording of each new sample reading. A more detailed sampling methodology is outlined in Boodoo et al. (2017, 2019).

2.3. DOC Concentration and DOM Composition

All samples for DOC concentration and DOM composition were stored on ice in a closed container until filtration through a double layer of Whatmann GF/F filters (within 6 hr of sample extraction). Filtered samples were stored at 4°C in the dark until analysis (within 48 hr). We used a GE Sievers 900® TOC analyzer to determine DOC concentrations and ultrapure water (MilliQ®) as the blank reference for both DOC concentration and DOM composition samples. DOM absorbance was measured in 5 cm cuvettes using a

Table 1
Characteristics of the Identified Fluorescent Components (C1–C5) Compared to Previously Identified Components

PARAFAC component	Excitation peak (nm)	Emission peak (nm)	Description
Component 1	260 (310)	410	UVA humic peak, of terrestrial origin, present in forest streams and wetlands (Stedmon & Markager, 2005; Fasching et al., 2016)
Component 2	260 (365)	478	Ubiquitous humic substances likely of terrestrial sources (Cory & Kaplan, 2012; Fasching et al., 2016)
Component 3	270	296	Tyrosine-like FDOM (Parlanti et al., 2000)
Component 4	260 (280)	348	Tryptophan-like FDOM (Coble, 1996; Fasching et al., 2016)
Component 5	275	304	Tyrosine-like FDOM (Coble, 1996)

Note. Fluorescent components were modeled by parallel factor analysis (PARAFAC) from excitation emission matrices. Excitation peak (nm) values in brackets represent secondary peaks.

UV-VIS spectrophotometer (Shimadzu UV-1700®). We calculated the slope ratio (S_R) as the ratio of $S_{275–295}$ to $S_{350–400}$ from absorbance spectra. The S_R has been found to inversely correlate with DOM molecular weight (Helms et al., 2008). The specific UV absorption ($SUVA_{254}$) was calculated as the absorption coefficient at 254 nm (m^{-1}) relative to the DOC concentration (mg L^{-1}) (Weishaar et al., 2003) and is an indicator of DOM aromaticity.

Furthermore, excitation emission matrices (EEMs) ranging from excitation (wavelengths: 240–450 nm) (5 nm increments) and emission (wavelengths: 270–550 nm) (2 nm increments) were generated using a Hitachi F-7000® fluorescence spectrophotometer and 1 cm quartz cuvettes. We corrected all EEMs for the inner filter effect and blank sample fluorescence using MilliQ® fluorescence measurements. EEMs were expressed in Raman units using the Raman peak of MilliQ® as a reference value. The humification index (HIX), as an indicator of the extent of sample humification, was calculated according to Zsolnay et al. (1999). The freshness index (β:α) as an indicator of the contribution of recently produced DOM compared to more decomposed DOM was calculated according to Parlanti et al. (2000). The fluorescence index (FI) as an indicator of the source of DOM was calculated according to McKnight et al. (2001). We also modeled DOM composition in terms of individual fluorescent components by parallel factor analysis (PARAFAC) (Stedmon & Bro, 2008) using the DOMFluor Toolbox Version 1.7 (Andersson & Bro, 2000). PARAFAC of OSB samples identified the presence of five distinct fluorescent components: Components 1 (C1) and 2 (C2) resembled humic-like fluorescence, while Components 3–5 (C3–C5) resembled protein-like fluorescence, likely from autochthonous sources (Figure 1c and Table 1). All components were expressed as percentages by standardizing each component by the total fluorescence of the sample.

2.4. Stream Corridor Hydrodynamics

In order to determine whether DOM composition within the OSB GB and SC was the result of only hydrodynamic drivers, that is, the simple mixing of hyporheic end-members—SW and GW, we employed an end-member mixing analysis approach. Expected DOM composition and concentration within the GB and SC were calculated based on mixing ratios of SW and GW (end-members). As GW EC was significantly higher than that of the GB locations, SC, and SW across all seasons (t test, $p < 0.001$, $n = 13–23$ for all seasons and location comparisons to GW), we utilized EC as a conservative tracer and determined SW and GW mixing ratios at each sampling site using the equations:

$$EC_{sample} = (EC_{SW} \times \%SW) + (EC_{GW} \times \%GW),$$

$$\%SW = \left[\left(EC_{sample} - EC_{GW}\right)/\left(EC_{SW} - EC_{GW}\right)\right] \times 100\%GW = 100\% - \%SW.$$

Expected DOM parameter values were calculated as the product of each end-member's percentage contribution to the sample composition and the observed DOM parameter value of the end-member, as outlined below:

$$DOC_{GB\ location} = [(DOC_{SW} \times \%SW_{GB\ location}) + (DOC_{GW} \times \%GW_{GB\ location})]/100$$

We plotted the expected seasonal average and standard error of the mean for key DOM values against those observed, determining whether DOM composition differed from that predicted by hydrodynamic mixing only.

Further investigating the effect of hydrology and DOM temporal variability, we utilized subsurface flow path and residence time (water age) data for the GB from Boodoo et al. (2019), corresponding to our current study period to determine whether residence time influences DOM composition within the OSB. Using a linear regression approach, we modeled residual DOM component and index values (based on the SW-GW mixing model above) against residence time (measured in days), calculated using the MIN3P model (Boodoo et al., 2019). Residence time was defined as the time taken for a downwelling parcel of water to arrive at a given sampling point from the initial location of downwelling into the streambed. DOM residuals were calculated as the difference between the observed and expected DOM parameter values—using the equations above. Thus, positive residual values (observed > expected) indicated production or lower than expected removal of a given DOM constituent and negative residuals (observed < expected) higher than expected removal or a decrease in the predicted rate of production of a constituent. Residence time in the GW model only considered SW downwelling as SW was determined to be the predominant end-member component in terms of mass flow (Boodoo et al., 2019). As our aim was to understand the effect of residence time on GB DOM composition and concentration and since the SC shows distinct physicochemical characteristics compared to the GB locations (supporting information Table S1)—likely leading to differing hydrodynamics, DOM data from the SC were excluded from this analysis.

2.5. Statistical Analysis of Data

Using principal component analysis (PCA), we investigated DOM composition within the GB and its end-members. This included modeled PARAFAC Components 1–5 (C1–C5), S_R, freshness index (β/α), FI, HIX, and absorbance at 254 nm ($SUVA_{254}$), over the full period of sampling (Table S1). We used the first principal component (PC1) scores and individual DOM indices as indicators of variability between locations. More specifically, we extracted the scores from PC1 as a composite indicator of DOM composition and additionally focused our comparisons on five key DOM characteristics (C2, C3, C5, $SUVA_{254}$, and HIX), in addition to DOC concentration. Key DOM characteristics were selected based on their PC1 scores and characteristic ability to best describe different DOM properties. All analyses were carried out in the statistical environment R (R Core Team, 2017). Comparison of observed and expected DOC concentration and DOM index and component values determined from mixing model analysis (described above) was used to determine potentially significant differences in DOM quantity and composition over space and time, unaccounted for by hydrodynamic mixing of SW and GW.

The effect of hydrology and temperature as potential drivers of DOC concentration and composition variability were tested using Pearson's product moment correlation. Furthermore, we tested for spatial and temporal differences between individual GB locations within and across seasons using Analysis of Variance (ANOVA) after transforming the data to meet the requirements of variance homogeneity and normal distribution. Further investigating whether GB DOM varied on the diurnal scale, we compared diurnal maxima and minima for individual DOM indices and the percentage contribution of individual DOM components using our seasonal high-resolution data set (three seasons, three samplings per day - over 5 to 7 consecutive days; Figure 1b) using paired *t* tests. All significance levels for multiple comparison tests were corrected using Dunn-Sidak correction (Sokol & Rohlf, 1969). Seasonal changes in temperature and climatic factors can affect in situ temperature and thus temperature mediated processes, resulting in changes in DOC concentration and shifts in DOM composition. We utilized multiple linear regression analysis to investigate the effect of both discharge and temperature on DOC concentration and composition (PC1 score) within the OSB over the entire sampling period. Additionally, the slope of regressions was used to identify the magnitude and direction of influence of independent variable drivers on DOC concentration and DOM composition.

In order to identify shifts in DOM composition along dominating flow paths within the GB, we separated all GB sampling locations into groups of similar DOM properties using DOM composition data from our monthly sampling campaign, representing DOM properties over different seasons and discharges, using cluster analysis. We used the *hclust* function in the *base* R package (R Core Team, 2017) to group all GB and SC sampling locations over both sampling depths (GB_{up} and GB_{low}) into five distinct DOM classes. Seasonal hydraulic head contour maps representing the average hydraulic heads within the GB during each season were utilized to indicate major flow paths within the GB. This allowed the

Table 2
Spatial Variability of DOC Concentrations Within the GB, SC, Stream Water, and Groundwater

	DOC concentration		
Location	Summer	Autumn	Winter
Head	1.48 ± 0.40	1.44 ± 0.24	1.35 ± 0.12
Crest	1.30 ± 0.18	1.45 ± 0.30	1.32 ± 0.18
Tail	1.45 ± 0.30	1.49 ± 0.19	1.30 ± 0.10
GB avg.	1.38 ± 0.14	1.44 ± 0.11	1.32 ± 0.1
Side Ch.	1.78 ± 0.49	1.59 ± 0.37	1.45 ± 0.18
Stream water	1.26 ± 0.17	1.27 ± 0.13	1.25 ± 0.1
Groundwater	5.45 ± 1.81	3.77 ± 0.17	3.08 ± 0.23

Note: Shown are the DOC mean ± standard deviation for each sampling season.

identification of changes in DOM composition over horizontal and vertical space along likely seasonally consistent flow paths within the GB.

3. Results

Stream discharge during the sampling period ranged between 0.07 and 0.97 $m^3\ s^{-1}$, averaging 0.40 $m^3\ s^{-1}$ (median: 0.47 $m^3\ s^{-1}$) over 15 distinct discharges. Within the GB and SC subsurface, SW was the main contributor to the hyporheic zone, with notable, but highly transient GW contributions at some GB locations. GW contributions ranged between 1.1% and 10.1% within the GB and 10.6% to 25.5% within the SC. GW contributions to hyporheic mixing decreased steadily from summer toward winter throughout the GB. Meanwhile, GW fluxes to the SC were substantially lower in autumn, compared to more similar and higher GW contributions at the SC in summer and winter (Table S2). GW spatial variability across the GB was generally lowest in autumn and highest in summer, as was the case for intraseasonal variability (as indicated by the standard deviation of the mean) at the individual GB and SC sampling locations (Table S2).

3.1. Spatiotemporal Patterns in DOC Concentration

DOC concentrations (Table 2) within the GB ranged from 1.03 to 3.31 mg L^{-1} (mean: 1.39 ± 0.25 mg L^{-1}), within the SC from 1.21 to 4.02 mg L^{-1} (mean: 1.60 ± 0.39 mg L^{-1}), and the OSB SW from 1.04 to 1.64 mg L^{-1} (mean: 1.26 ± 0.13 mg L^{-1}). Furthermore, riparian shallow GW DOC concentration was consistently more than double that of the GB, SW, and SC across all seasons, ranging from 2.41 to 7.54 mg L^{-1} (mean: 3.54 ± 0.75 mg L^{-1}). SW DOC concentration was significantly lower than the GB (average of GB head, crest, and tail) and the SC across all seasons (*t* test Bonferroni corrected for multiple comparisons, $p < 0.05$, $n = 21$ to 24 for all comparisons), except during summer within the GB (*t* test, $p = 0.08$, $n = 14$).

DOC concentration varied significantly (ANOVA: $p < 0.001$) across seasons at all sampling locations with the exception of the GB head and SW. Interseasonal DOC comparisons (Pairwise Tukey honestly significant difference) between DOC concentrations at each sampling location revealed variability in seasonal differences among the different sampling locations (Figure S1). Investigating DOC variability between GB and SC sampling depths (GB_{up} and GB_{low} and SC_{up} and SC_{low}, respectively), we found GB_{up} and SC_{up} DOC concentrations to be generally significantly higher than GB_{up} and SC_{up}, respectively, during summer and autumn (*t* test, $p < 0.05$, $n = 18$ to 24 for all comparisons) but not winter. The GB crest was the only location which consistently showed no variability in DOC concentration over depth (Table S3).

DOC concentration was typically higher than predicted by SW-GW mixing at all GB sampling locations except the GB head during autumn, while during summer, observed DOC concentrations were typically lower than expected. During winter, observed DOC concentration was similar to that predicted by our SW-GW mixing model. Along the SC, DOC concentration was substantially lower than predicted during summer and winter, while during autumn, DOC concentrations were more similar to that predicted by simple SW-GW mixing.

3.2. Spatial and Temporal Patterns in DOM Composition

In order to better understand DOM dynamics beyond DOC concentration, we investigated DOM composition (derived from absorbance and fluorescence measurements, HIX, $SUVA_{254}$, FI, β/α, and S_R) and the proportion of DOM components (modeled by PARAFAC analysis), over space and time. PARAFAC analysis identified a total of five DOM components. The two humic-like components, C1 and C2, most resembled those identified by Coble (1996) as Fluorophores A and C, respectively, while the three protein-like components (C3–C5) most resembled tyrosine-like fluorescence and tryptophan-like fluorescence (Figure 1c and Table 1), corresponding to recently produced DOM of microbial origin. The fluorescence of C3 and C5 may both represent tyrosine-like fluorescence, as indicated by their similarity to components identified as tyrosine-like in previous studies (Coble, 1996; Fasching et al., 2016; Parlanti et al., 2000). However, biogeochemical processes, such as biological degradation and photooxidation, have been shown

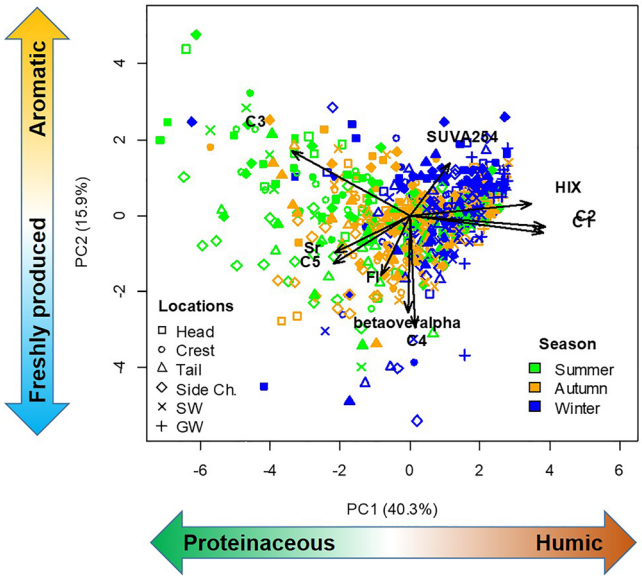

Figure 2. Principal component analysis (PCA) based on absorbance and fluorescence measurements of GB subsurface porewater, stream water and groundwater. Humic-like fluorescence (C1 and C2), protein-like fluorescence (C3–C5), specific absorption at 254 nm ($SUVA_{254}$), humification index (HIX), fluorescence index (FI), freshness index (ß/α), and slope ratio (S_R) are shown. Arrow lengths are based on PCA structural coefficients. PCA hollow symbols represent GB_{up}/SC_{up}, while filled symbols represent GB_{low}/SC_{low}. Points are colored by sampling season: summer = green, autumn = orange, winter = blue.

to shift fluorescence maxima (Hansen et al., 2016; Hudson et al., 2007), leading to the differentiation of DOM components. This may have occurred within the OSB as the tyrosine-like component transits through the GB. Additionally, DOM components sharing similar optical properties may represent different sources of DOM (Hansen et al., 2016), such as stream algal exudates, streambed surface biofilms, or subsurface sediment biofilms within the GB itself.

PCA analysis of DOM composition across all sampling locations revealed an overall distinct gradient from relatively autochthonous DOM to more terrestrial DOM with increasing stream discharge (Figures 2 and S2). The first two PC axes (PC1 and PC2) together explained the majority (56.2%) of variability in DOM composition within the OSB stream corridor over the three different sampling seasons. PC1 explained 40.3% of all DOM variability and showed DOM composition to be seasonally variable (Figure 2). The gradient in DOM composition ranged from more protein-like and less complex (protein-like component C3 and C5, low molecular weight—S_R) DOM in summer to more humic-like and more complex (higher percentage of the humic-like components C1 and C2, higher HIX) DOM in winter (Figure 2). PC2 explained 15.9% of all DOM variability. PC2 represented a gradient from more complex, aromatic (higher $SUVA_{254}$) DOM to more freshly produced and labile DOM (more protein-like DOM [C4], higher freshness index). PC2 scores decreased from summer toward winter, indicating an increase in prevalence of more aromatic DOM. This pattern was not consistent during a period of higher flow which resulted in more recently produced DOM of likely microbial origin (high freshness index and FI). The PCA also revealed higher contributions of aromatic DOM within the stream and GB_{up} and SC_{up} during summer.

Overall, the GB head, tail, and SC showed the highest degree of protein-like contributions to the DOM pool across all seasons, while GW DOM remained aromatic and humic-like across all seasons (Figure 2). DOM composition of the GB locations, as well as along the SC, varied across the individual sampling seasons (ANOVA, $p < 0.001$ for all comparisons), with a more protein-like character and smaller apparent molecular weight (lower PC1 values) in summer, toward a more aromatic and humic-like character (higher PC1 values) in winter (Figure S1). The GB crest and SC were the only locations where DOM composition varied significantly across all three sampling seasons (Table S3, post hoc Tukey HSD, $p < 0.05$).

GW DOM composition was distinct (*t* test, $p < 0.001$ for all comparisons) from that of the other sampling locations (GB, SC, and SW) across all seasons, showing a higher PC1 value—stronger humic character, with high HIX and $SUVA_{254}$ values and a higher occurrence of the humic-like components C1 and C2 (Figure 2). Seasonal DOM variability, as indicated by the standard deviation of PC1 scores (gradient of protein-like to humic-like DOM character) for all GB locations (head, crest, and tail), the SC, and SW, consistently decreased from summer toward winter, while variability in DOM composition of the GW increased (Figure S1).

While DOM composition, represented as the PC1 score, did not significantly vary between the GB and the stream (*t* test, $p > 0.05$ for all comparisons), comparisons of individual indicators of DOM composition within the GB and SW showed significant differences. Within the GB, DOM composition, as represented by C5 (all seasons) and C3 (winter only), significantly differed from that of SW (Mann-Whitney U test, $p < 0.05$, $n = 14$ to 24 for all comparisons). Meanwhile, HIX and $SUVA_{254}$ within the GB did not differ significantly from the SW (Mann-Whitney U test, $p > 0.05$, $n = 14$ to 24 for all comparisons). Furthermore, DOM composition exhibited a clear diurnal pattern within the GB, SC, and SW (paired *t* test, $p < 0.05$, $n = 5$ to 7) during autumn and winter as represented by marked differences in diurnal maxima and minima in selected PARAFAC components (C2, C3, and C5) and indices (HIX and $SUVA_{254}$). However, diurnal maxima and minima of DOM indices and DOM concentration were not statistically distinguishable during summer months (Figures 3 and S3).

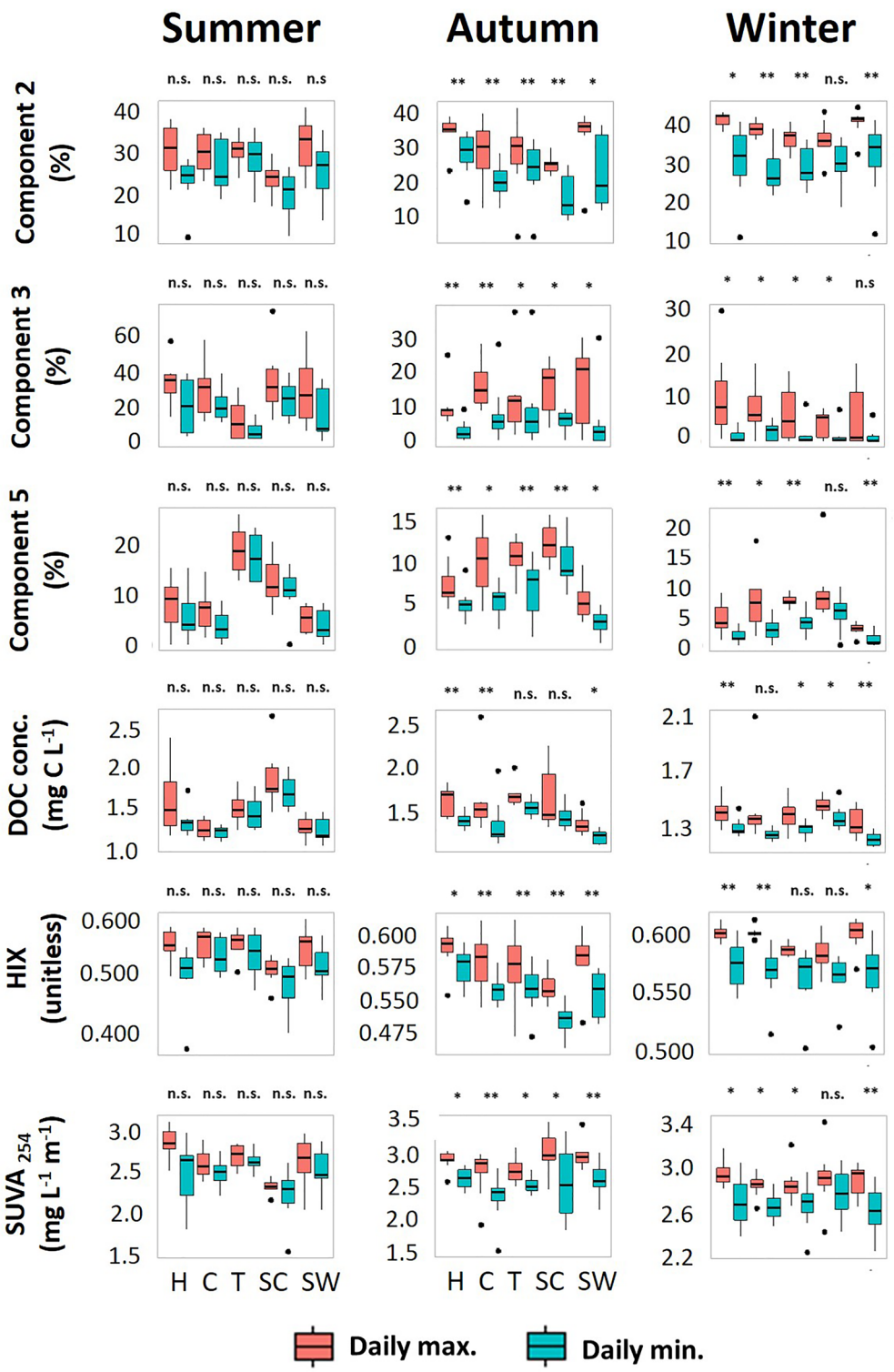

Figure 3. Boxplots showing the variability of daily maxima and minima for selected DOM characteristics within the upper permanently wetted section (GB_{up}) of the GB head (H), crest (C) tail (T), and SC (SC_{up}), as well as stream water (SW) sampling locations, during different seasons: summer, autumn, and winter (five to seven sampling points per location). Star notation indicates statistical difference between seasonal daily minimum and maximum DOM parameter values for each location (paired *t* test), where * = $p < 0.05$, ** = $p < 0.01$, *** = $p < 0.001$, and ns = no significant difference ($p > 0.05$).

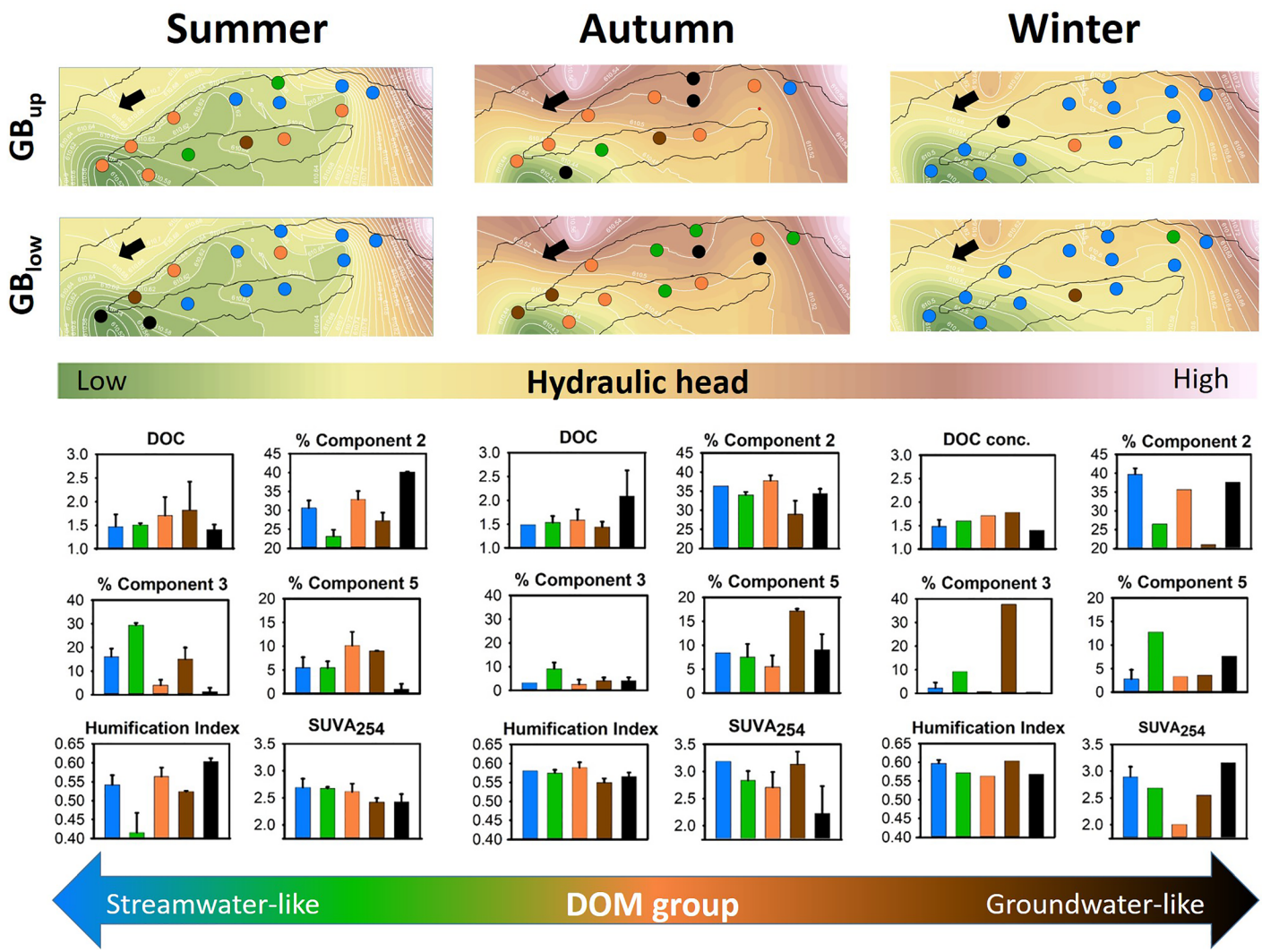

Figure 4. Seasonal variability in DOM characteristics across GB_{up} and GB_{low} and SC_{up} and SC_{low}. DOM groups represent GB and SC locations showing similar seasonal DOM properties as determined by cluster analysis of seasonal DOM composition parameters and indices. Contour shading (contour lines plotted at 2 cm intervals) corresponds to the respective seasonal average hydraulic head values measured within the GB and SC. Bar plots show seasonal average DOM composition indices and DOC concentration for each DOM group. Bar plot height and error bars show DOM index average and standard deviation. Black lines and arrows indicate the GB outline and stream water flow direction, respectively. DOM components (C2, C3, and C5) are shown in percentage occurrence (%), DOC = mg C L^{-1}; $SUVA_{254}$ = mg L^{-1} m^{-1}; and HIX = unitless.

Investigating further the spatial variability of DOM, we used cluster analysis to identify locations which were similar in DOM composition, identifying five distinct DOM groups among the various GB and SC sampling locations (Figure 4). Locations of strong downwelling along the upstream perimeter of the GB were consistently associated with Group 1 (Figure 4), suggesting it represented SW-like DOM. The classification of Group 1 as SW-like was supported by its comparatively low DOC concentration and high $SUVA_{254}$ and HIX (Figure 4). Overall, DOM composition increasingly shifted away from an apparent SW-like composition (Group 1) on moving from the upper GB to the lower GB along presumed downwelling flow paths (inferred by hydraulic head contour patterns). Downwelling SW moving along hydraulic gradients tended to increase in protein-like (%C3 and %C5) DOM and DOC concentrations and decrease in aromaticity ($SUVA_{254}$). The occurrence of the Group 5 coincided with a region of shallow GW upwelling identified during summer low flow conditions by Boodoo et al. (2019) while that occurring during higher discharge in winter coincided with a region of upwelling identified by Battin (1999), suggesting Group 5 likely represents GW-like DOM. Thus, DOM Groups 2 to 4 likely represented locations of notably different DOM composition compared to the stream and GW, with changes in DOM composition resulting from biogeochemical processes

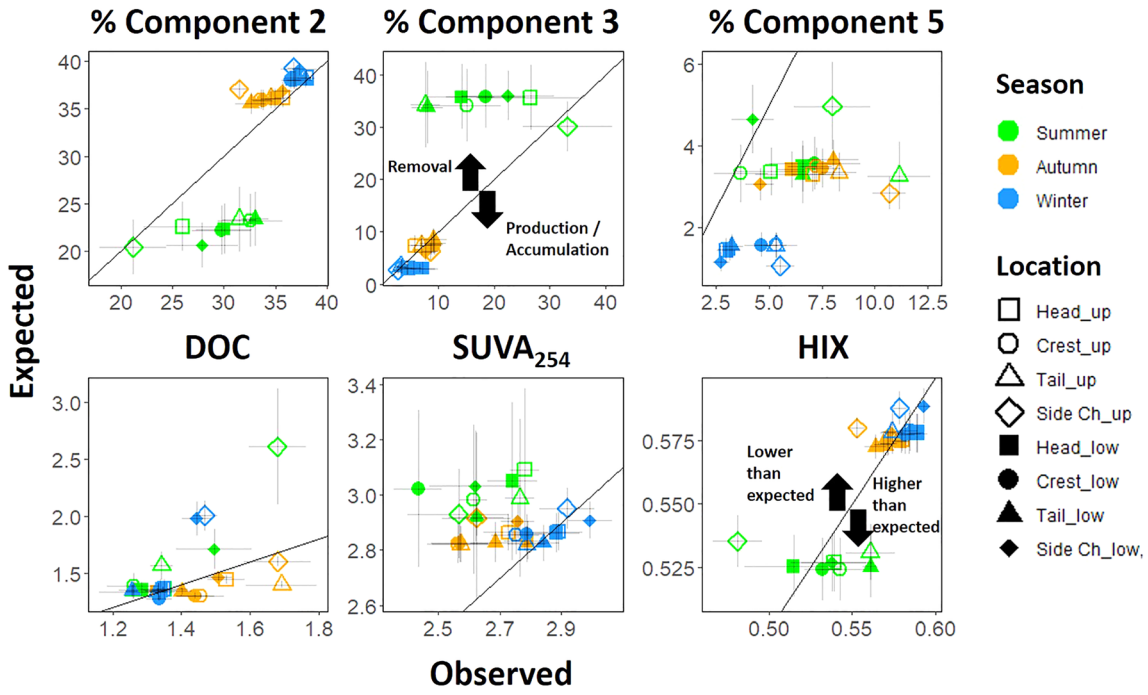

Figure 5. Plots showing observed versus expected seasonal average GB and SC DOM parameter values. The solid line represents the 1:1 line. Points above the 1:1 line indicate removal or lower than expected production, while points below the line indicate the production or lower than expected removal (accumulation) of the DOM component or parameter. Error bars represent the standard error of the mean for each seasonal average point in order to account for slight differences in sample numbers across the different locations and seasons. Expected values for each GB location (and parameter) were calculated from mixing model analysis, based on the conservative mixing of GB hydraulic end-members: stream water and groundwater. DOM components (C2, C3, and C5) are shown in percentage occurrence (%), DOC = mg C L^{-1}; $SUVA_{254}$ = mg L^{-1} m^{-1}, and HIX = unitless.

within the GB and/or the physical mixing of distinct SW and GW within the GB subsurface. Furthermore, with the exception of in winter, DOM groups tended to shift away from Groups 1 and 5 moving along presumed flow paths (Figure 4).

The pattern of DOM variability within the GB and SC appeared to be related to seasonal differences in stream hydrology. Prevalence of apparent SW-like DOM composition throughout the GB and SC was highest in winter and lowest in autumn. The DOM composition of the most upstream section of the GB (Figure 4), perpendicular to the stream flow, remained most SW-like throughout all seasons, while the tail and SC, locations with typically higher EC (Table S1), were more GW-like. Furthermore, high levels of C3 along the GB perimeter and SC were closely associated with sites of water pooling and their presumed flow path based on downwelling along identified hydraulic gradients within the GB. Together, these patterns suggest a progressive shift in DOM composition of downwelled SW within the GB along downwelling flow paths (Figure 4), highlighting possible hydrodynamic and biogeochemical controls on interseasonal and intraseasonal heterogeneity in DOM composition.

3.3. DOM Removal and Transformation Within the GB

In situ temperature (as an indicator of season), in addition to stream discharge (representing the effect of SW-GW mixing), significantly explained 10.9%, 3.4%, 10.3%, and 54.5% of observed variability in DOC concentration across the sampling year at the GB head and tail and the SC and GW, respectively (multiple linear regression, model $p < 0.05$). However, the model could not explain the observed variability in DOM composition at the GB crest and within SW (Table S4). In contrast, DOM composition (as represented by the PC1 scores) could be significantly predicted by in situ temperature and stream discharge (Table S5) across all sampling locations. These two predictors explained a total of 22.1%, 30.1%, and 14.3% of DOM variability at the GB head, crest, and tail, respectively. Meanwhile, 16.6%, 30.2%, and 10.9% of DOM variability within the SC, SW, and GW was explained by discharge and temperature during sampling (Table S5).

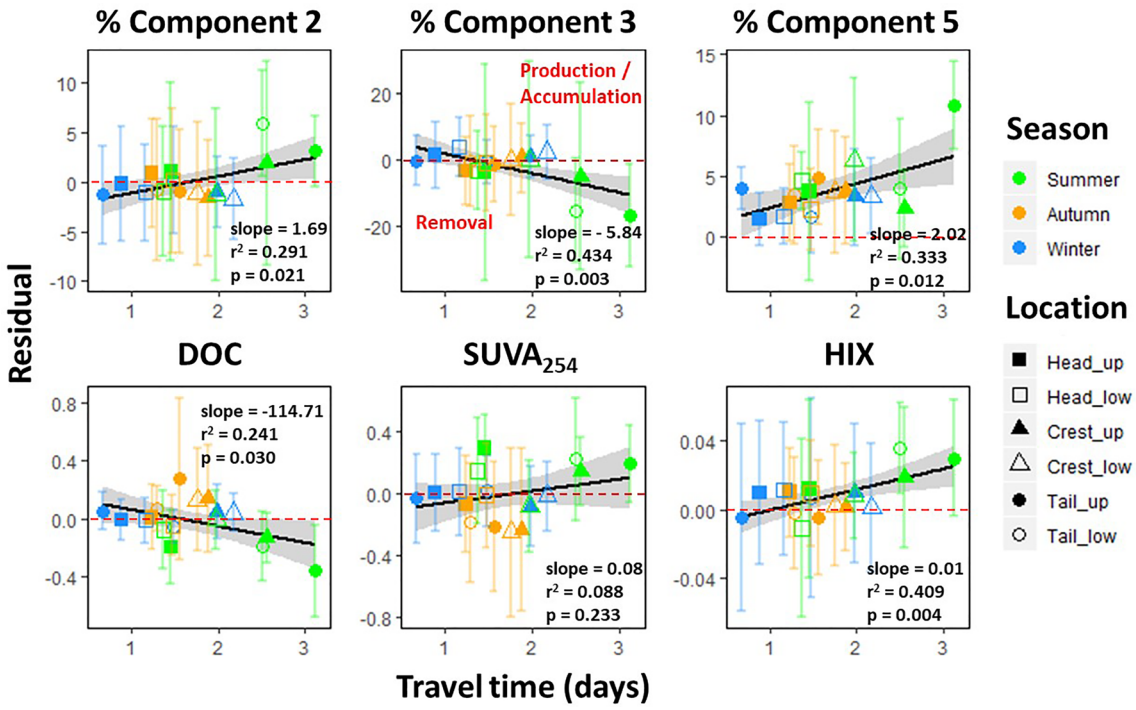

Figure 6. Plots showing seasonal average residuals (observed-expected) of the stream water-groundwater mixing model for major DOM parameters versus residence time. Residence time is the amount of time taken from the moment at which a parcel of water has downwelled from the stream into the streambed/GB subsurface to that at which it arrives at the respective point of sampling. Positive sloped relationships indicate an increase in positive DOM parameter residual (production or decrease in removal rate of DOM) with increasing residence time, while a negative slope indicates a decrease in DOM parameter residual (removal or decrease in production rate of DOM) with increasing residence time. Points above and below the 0.0 residual point on the *y* axis represent relationships where the residual is positive (higher than expected DOM values) and negative (higher than expected DOM values), respectively. Error bars represent the standard error of the mean for each point. The shaded area around the best fit line indicates the confidence intervals of the linear model. DOM components (C2, C3, and C5) are shown in percentage occurrence (%), DOC = mg C L^{-1}; $SUVA_{254}$ = mg L^{-1} m^{-1}; and HIX = unitless.

Further investigating the effect of discharge on variability of individual indicators of DOM composition, we found that within the GB, SC, and SW, higher flows (occurring mainly in winter) coincided with increased aromatic character as indicted by HIX (Pearson's product moment correlation: 0.64, 0.68, and 0.38 respectively) and humic DOM (C2) character of DOM (Pearson product moment correlation: 0.66, 0.66, and 0.44, respectively). Meanwhile, lower flows and summer baseflow were closely associated with increased %C3 (Pearson's product moment correlation: 0.62, 0.55, and 0.45 at the GB, SC, and SW, respectively).

In order to determine whether observed shifts in DOM composition (Figure 4) were the result of simple SW-GW mixing or biogeochemical activity within the GB, we used a mixing model approach. DOM composition within the GB and SC deviated distinctly from that predicted by the mixing of its end-members—SW and GW (Figure 5). The highest deviation in DOM character from that expected by SW-GW mixing was observed in summer (*t* test, $p < 0.05$, $n = 79$ to 106, for all selected parameters except HIX), decreasing in autumn (*t* test, $p < 0.05$, $n = 79$ to 106, for all selected parameters except for C3) and winter (*t* test, $p < 0.05$, $n = 79$ to 106, for all selected parameters except for HIX and $SUVA_{254}$). This pattern was mainly driven by elevated contributions of the humic-like component C2, while the protein-like components C3 was lower and C5 (with exception of the SC) higher than expected. Furthermore, the protein-like component C5 was consistently higher and $SUVA_{254}$ (with the exception of during winter) lower than expected (Figure 5).

To identify whether residence time within the GB was a significant driver of DOM transformation, we investigated the relationship between residence time within the GB (Table S1) and the residuals of DOC concentration and DOM composition derived from our mixing model (Figure 5). The use of residual DOM values corresponding to hydrological conditions during each sampling period allowed for the determination of DOM changes within the GB that were not a result of SW-GW mixing but GB processing and removal. A

positive or negative relationship between DOM concentration/composition and residence time therefore indicates the production/accumulation or removal of the respective fractions of DOM, along flow paths within the GB itself (Figure 6).

Within the GB, we found residence time to be a significant driver of DOM quantity and composition shifts, particularly during summer, highlighting the role of hydrology on DOM dynamics in GBs. Our analysis of the effect of residence time excluded the SC, based on its lower hydraulic conductivity (4 times lower than the GB average; Boodoo et al., 2017, 2019) and the fact that residence times for the OSB hyporheic zone were calculated specifically for the GB (head, crest, and tail) using the GB average sediment conductivity (Boodoo et al., 2019), likely leading to inaccurate SC residence times. Notwithstanding this, estimated residence times (up to an order of magnitude higher than the GB; Figure S5) in the SC were associated with low oxygen concentrations (Table S1), suggesting limited potential for DOM processing via aerobic microbial processing, compared to the GB. Shorter residence times within the GB during autumn and winter appeared to result in limited changes in residual mixing model DOM properties, while higher residence times in summer led to clear temporal shifts in DOM residuals (Figure 6). Increasing residence time led to a significant decrease in residual DOC concentration (linear regression: $p < 0.05$, slope $= -0.115$ mg C day^{-1}). Furthermore, increasing residence time resulted in decreased occurrence of C3 (linear regression: $p < 0.01$, slope $= -5.84\%$ C3 day^{-1}) residuals and an increase in percentage occurrence of C2 (linear regression: $p < 0.05$, slope $= 1.69\%$ C2 day^{-1}) and C5 (linear regression: $p < 0.05$, slope $= 2.02\%$ C2 day^{-1}) and higher HIX (linear regression: $p < 0.01$, slope $= 0.01$ day^{-1}) residuals (Figure 6).

4. Discussion

GBs act as sites of elevated DOC processing (Vervier et al., 1993) and removal (Findlay et al., 1993; Findlay & Sobczak, 1996) within stream and river corridors. DOM dynamics within streams have been shown to be influenced by seasonal shifts in discharge, temperature, and phenological events (e.g., Fasching et al., 2016; Singh et al., 2014). Furthermore, while DOM processing within intermittent streams and their streambed during drought conditions has been recently investigated (Harjung et al., 2018), the transformation and removal of DOM within GBs during periods of flow and over different seasonal conditions remain elusive. Here we examined the role of hydrodynamic exchange between SW and shallow GW, as well as related residence time and temperature for DOM transformation within a GB across seasons. We identified significant spatial and temporal variability in DOM quantity and composition within the GB, differing from that predicted by the mixing of SW and GW. We attribute these shifts in DOM concentration and composition to the transformation and removal of DOM along hydrological flow paths within the GB.

4.1. DOM Sources and Composition

DOC concentration and DOM composition showed high variability over seasons within the GB, SC, and adjacent GW and SW. GB and SC DOC concentrations responded to shifts in seasonal drivers, with higher DOC concentrations during summer and autumn, when subsurface temperatures and GW inputs were noticeably higher, while SW DOC concentrations did not vary across seasons. At the same time, DOM composition within the GB, SC, and SW shifted from a more humic-like composition in winter, toward a more protein-like composition in summer and autumn, highlighting variable responses in DOM concentration and composition to shifts in seasonal drivers. Seasonal controls on temperature and light regimes can influence the production and release of algal exudates (Kaplan & Bott, 1982), particularly during summer low flows (Inamdar et al., 2011) likely impacting the concentration and composition of the DOM pool within the GB. We identified the protein-like DOM Component C4, associated with DOM of increased FI and freshness index values (not shown), as likely originating from biofilm and algae present on fallen leaves and streambed sediments (Figure 1d). This matches the tryptophan-like component C4—showing elevated freshness and FI values and maximum values during summer baseflow, found in the OSB stream and hyporheic waters by Fasching et al. (2016). Similarly, autochthonous DOM contributions from benthic biofilms and primary production have been shown to influence DOM composition (Kaplan & Bott, 1989), particularly during summer months when temperatures and PAR are high, as was observed at the OSB SW, GB head, and SC (Figure 1a). Furthermore, photooxidation of DOM within the stream and exposed pools can lead to decreases in DOM complexity (Fasching & Battin, 2011; Helms et al., 2008), with potential consequences for DOM bioavailability and DOM processing (Kragh et al., 2008). High levels of

photooxidation during summer and autumn would explain our finding of significantly higher S_Rs within the stream and areas of increased SW downwelling within the GB and SC during summer and autumn, but not in winter.

Peak DOC concentrations and FI (not shown) observed within the stream, SC, and GB during autumn were likely linked to leaching of protein-like DOM from leaves entrained at these locations. Sites where high protein-like and autochthonous DOM occurred corresponded to sites of water pooling and higher residence time—the SC and a pool near the GB head, increasing opportunity for photooxidation and microbial processing. Autumn leaf fall can be associated with increased protein-like fluorescence and can play a major role in seasonal shifts in DOM quantity and composition (Singh et al., 2014). In fact, protein-like fluorescence has been associated with leaf-leachate, algal-derived DOM and hyporheic microbial production, representing a source of labile DOM (Wong & Williams, 2010). Thus, it is likely that leaching of leaf litter in autumn provided a readily available terrestrial protein-like DOM source for GB hyporheic microbial processing in autumn.

Hyporheic hydrodynamics, influencing SW-GW mixing and residence time within the GB and SC subsurface, acted as a strong control on hyporheic DOM dynamics. Higher GW upwelling fluxes in summer and autumn corresponded with lower SW downwelling velocities and higher hyporheic residence time compared to winter (Boodoo et al., 2019). Thus, hyporheic hydrodynamics, controlling GW fluxes, may have acted as a major source of variability in DOM composition within the GB and SC, particularly in summer. However, GW DOC concentration within the OSB was consistently higher than all other sampling locations and continually contributed humic and more aromatic DOM to the GB. The high levels of the humic-like components C1 and C2 observed within the GW likely resulted from the enrichment by soils in the riparian forest surface horizon (Aitkenhead-Peterson et al., 2007). While GW DOC concentration significantly decreased from summer toward winter, contributing to overall hyporheic DOM seasonal variability, we found GW DOM composition not to vary, with DOM composition remaining humic-like throughout all seasons. These muted seasonal dynamics of GW DOM within the GB may be attributable to the loss of DOM by sorption onto mineral soil surfaces and/or microbial processing (Singh et al., 2014).

In contrast to summer and autumn, higher SW discharge in winter resulted in lower residence times and increased SW downwelling within the GB. As a result, higher SW downwelling velocities and lower residence times in winter led to dominance of the GB and SC sediments by SW, reflected by the absence of significant differences in DOM composition among the stream and GB and SC. However, while discharge within seasons was relatively constant, an increased flow event (Figures 2 and S2) caused a temporary shift of DOM composition during winter toward a more proteinaceous signal and an increase in the amount of more freshly produced DOM. Singh et al. (2014) observed a similar increase in labile DOM during spring, attributing the shift in DOM composition to the hydrologic flushing of accumulated soil DOM into the stream. This may indicate that hydrologic flushing of accumulated labile DOM, potentially derived from benthic biofilms (Kaplan & Bott, 1989), may also play an important role within GBs.

4.2. DOM Diurnal Variability

DOC concentration and DOM composition within the GB varied on a diurnal scale except during summer when diurnal maxima and minima of DOM indices and DOM concentration were not statistically distinguishable, suggesting seasonal controls on diurnal variability. Diurnal variability of DOC concentration and DOM composition within streams have been previously linked to photooxidation of DOM (Fasching et al., 2016; Spencer et al., 2007), resulting in reduction of DOM complexity and lability (Helms et al., 2008) and the in-stream production of more labile proteinaceous DOM via algal photosynthesis (Kaplan & Bott, 1989). As the studied section of the OSB has been shown to be predominantly losing, resulting in SW downwelling into the hyporheic zone exceeding upwelling hyporheic and GW fluxes, particularly during low flows (Battin, 1999; Boodoo et al., 2017), diurnal patterns in SW DOM variability, though lagged and/or attenuated, were transferred into the GB and SC hyporheic zone.

While GB DOM characteristics varied diurnally within the GB and SC, the timing of daily maxima and minima shifted throughout the day (except at the GB crest), highlighting a decoupled relationship with DOM variability within SW which showed a clearer day-night rhythm (data not shown). Similarly, lagged diurnal SW CO_2 peaks were observed to occur within the GB (Boodoo et al., 2017). Differing

lagged/attenuated SW DOM patterns within the GB and SC were likely in response to physical controls on subsurface hydrodynamics as a result of differences in GB sediment hydraulic conductivity. In fact, hydraulic conductivity at the GB crest was found to be notably higher than that of the other sampling locations and the GB crest to have similar physicochemical characteristics and CO_2 outgassing rates to that of the SW (Boodoo et al., 2019). Similarly, lagging effects and attenuation of SW thermal signals were shown to occur within the hyporheic zone of a gravel-/cobble-bed stream in Oregon, USA, by Arrigoni et al. (2008), with the magnitude and pattern of variability dependent on the degree of hyporheic exchange. These findings point to hyporheic hydrodynamics—controlling hyporheic exchange, as an important determinant of DOM diurnal variability and possibly also temperature, within GBs.

It is interesting to note that we did not observe a significant diurnal signal in DOM concentration nor its composition within the stream or GB and SC, when diurnal PAR and temperature differences were the highest. This overall lack of diurnal variability during summer could be the result of higher inputs of compositionally stable GW in summer, masking DOM diurnal variability within the stream and hyporheic zone. Similarly to our findings, consistent GW terrestrial inputs have been reported to blur temporal patterns in the autochthonous fraction of DOM within the hyporheic zone (Fasching et al., 2016). Furthermore, increased microbial uptake of autochthonous DOM, promoted by lower SW downwelling velocities—increasing hyporheic residence time and higher sediment temperatures in summer, may have contributed to the absence of diurnal DOM signals within the GB and SC.

4.3. Vertical Patterns of DOM Concentration and Composition

We found higher DOC concentrations within the GB and SC sediment, compared to the OSB stream, with DOC concentrations decreasing with sediment sampling depth. These findings are supported by those of Battin (1999, 2000) who observed the same patterns within the OSB bed sediments. In contrast to our findings, Fasching et al. (2016) showed for the same study location that SW DOC concentration within the OSB was in fact higher than the streambed hyporheic zone. This was likely the result of the greater depth of hyporheic sampling (1.5 m below streambed surface) conducted during investigations by Fasching et al. (2016) compared to that in the current study (GB_{up} and GB_{low}) and studies conducted by Battin (1999, 2000) in the same location (0.3, 0.5, and 0.75 m below streambed surface). This points to increased removal of DOC via hyporheic biological and/or physicochemical processes as depth increases within the GB. In fact, several studies have shown that the upper shallow interstitial sediment layer effectively removes DOC, with concentrations rapidly decreasing with increasing depth (Battin et al., 2003; Hendricks & White, 1991; Marmonier et al., 1995). In fact, the maxima of total organic carbon concentration for the OSB was reported to occur between 20 and 40 cm depth below the streambed surface (Leichtfried, 1988), corresponding to our sampling location GB_{up}, located ~15 cm below the GB summer baseflow hyporheic water level. Such patterns of declining DOC concentration with increasing hyporheic depth have been attributed to the rapid degradation of BDOC by hyporheic microbial communities in downwelled oxygen rich waters within the hyporheic zone in the White Clay Creek, Pennsylvania, USA (Battin et al., 2003). Furthermore, DOC may become adsorbed onto sediment (Findlay & Sobczak, 1996; Hunter et al., 2016) or incorporated into biofilms (Battin et al., 2008) as it moves through the hyporheic zone, explaining the observed decrease in DOC concentration along downwelling flow paths within the GB.

Downwelling SW hydrodynamics likely controlled vertical DOM spatial variability as seasonal differences in DOM concentration and composition between GB_{up} and GB_{low} decreased from summer toward winter along with increased seasonal SW downwelling velocities (Boodoo et al., 2019). Slower and weaker SW downwelling during summer would facilitate increased microbial processing and removal of DOM along downwelling flow paths, leading to lower DOC concentrations and altered DOM composition within the lower hyporheic zone. Weaker SW downwelling facilitated greater SW-GW mixing, explaining higher DOC concentrations in the upper hyporheic zone. These patterns were further evidenced by higher specific EC within the upper GB sections compared to the lower GB (Table S1). In winter, when SW downwelling was the highest, this vertical gradient in DOM concentration and composition as well as EC collapsed, with DOM concentrations and composition across the GB and SC at both sample depths more similar to SW (Table S1). Furthermore, higher SW downwelling flow velocities (Boodoo et al., 2019) within GB_{low} could explain the significantly lower DOC concentrations—more similar to the stream, at this location when

compared to GB_{up} during summer and autumn. Considered together, these interseasonal and intraseasonal patterns highlight the occurrence of substantial rates of microbial processing and DOM removal at the bedform scale, as a result of small-scale, site-specific GB hydrodynamics.

4.4. DOM Transformation and Removal Along GB Flow Paths

We found that the GB to be a zone of increased biogeochemical activity, transforming and removing DOM received from its end-members (e.g., C2 and C3), promoting autochthonous DOM production (C5), while acting as an overall DOC sink. DOC was increasingly removed along the flow path with increasing residence time, with concurrent changes in DOM composition along identified flow paths (Figures 4 and 6). Downwelling of oxygen-rich SW, combined with warmer sediment temperatures, particularly within GB_{up} and SC_{up} sediment (Boodoo et al., 2017), likely promoted increased levels of microbial activity and biofilm growth during summer and, to a lesser extent, autumn. Additionally, increased GW inflow, acting as a source of DOC and nutrients in summer and autumn, and longer residence times may facilitate reactions altering DOM composition (Figure 5). This likely led to the removal of terrestrial DOM along GB flow paths, while autochthonous DOM was simultaneously produced within the GB. Contributions of protein-like component C5 particularly increased, suggesting production and/or relative removal of other DOM fractions. However, as the absolute values of C5 (R.u.) also increased, especially in autumn and winter, it is likely that C5 is produced within the GB (Figure S4). Removal of C5 during summer only may be linked to higher rates of microbial activity/removal within the GB during periods of warmer hyporheic temperatures and longer residence times, while lower temperatures and residence times allow for accumulation of C5. We propose therefore that the protein-like component C5 represented microbially derived protein-like DOM produced within the GB and the stream and/or GW. Furthermore, we observed the simultaneous removal of humic fractions (C1 and C2) with increased residence time in the GB and production of autochthonous DOM. At the same time, we observed overall lower $SUVA_{254}$ values, potentially indicating microbial degradation of the more aromatic DOM fraction (Fasching et al., 2014) within the GB. In fact, microbial processing of DOM in lakes and rivers can lead to the simultaneous consumption and production of DOM (Guillemette & Giorgio, 2012). Within our GB, labile DOM may originate from algal and benthic biofilm dissolution and transport within the GB or microbial lysis/release of labile DOM, in response to water level fluctuations (Stegen et al., 2016), impacting the wetted area and flow paths within the GB or microbial transformation of DOM received from SW and/or GW. Similarly, within the hyporheic zone of a Mediterranean stream, disproportionally high rates of DOM processing were shown to occur during drought conditions, with an initial period of autochthonous, protein-like DOM production, followed by an extended period of aromatic and high molecular weight DOM retention within the hyporheic zone (Harjung et al., 2018). This indicates that the observed production of autochthonous labile DOM and removal of more aromatic fractions within alpine GBs is not limited to alpine and perennial stream ecosystems but may occur in a wide range of hydrological and climatic ecosystems, supporting the regional and global relevance of our findings.

Longer residence times have been shown to correspond to increased levels of microbial processing and alteration of DOM within both the stream (Battin et al., 2008; Gooseff et al., 2011; Kaplan et al., 2008) and hyporheic zone (Briggs et al., 2013; Trulleyová et al., 2003), facilitating the conversion of more complex allochthonous DOM into more readily available labile components—fueling microbial respiration and production. During summer at the OSB, chlorophyll a and sediment carbohydrates explained more than 90% of the variance in shallow streambed microbial activity, with lower turnover times (factor of 3) in summer compared to autumn/winter (Battin, 2000). Furthermore, seasonal temperature differences (Table S1) can play a major role in controlling DOC dynamics, in terms of DOC dissolution and aquatic microbial respiration (Raymond & Spencer, 2015; Yvon-Durocher et al., 2012). Therefore, lower temperatures and lower residence times in winter, together with higher discharges, may limit the removal of less labile DOM of humic and aromatic character within the OSB. These seasonal shifts in decreasing temperature and reduced residence time may effectively suppress heterotrophic metabolism (Battin et al., 2008) and lead to predominantly hydrodynamic controls on DOM dynamics as predicted by our SW-GW mixing model during winter. Thus, it is probable that lower residence time and hyporheic temperatures during autumn and winter precluded clearly observable changes in DOM characteristics with increasing residence time. Furthermore, the removal of DOM within streams has been linked to its reactivity, whereby the labile fraction of DOM was removed from the stream in ~1.5 hr, while less labile DOM fraction had a turnover

of ~29 hr within the White Clay Creek catchment, USA (Kaplan et al., 2008). Assuming similar labilities and processing times within the GB, the most labile fraction of DOM within the SW can potentially be completely removed within the GB due to the relatively high residence time and short flow path lengths within the GB subsurface sediment during summer (Table S1). As inferred from our results, changes in DOM composition (relative to the stream) increased with higher hyporheic residence time within the GB subsurface, with an apparent critical residence time of ~2 days required for significant changes in DOM composition to be observed (Figure 6).

Overall, DOM composition within the studied GB showed substantial lateral and vertical variability, with DOM being simultaneously removed and produced along hyporheic flow paths. These processes were controlled by seasonal variability in discharge controlling SW-GW mixing and hyporheic residence times, along with changing seasonal temperature. Our findings highlight GBs as important sites of in-stream DOM processing. Understanding the role of GBs in processing DOM will help to gain an improved understanding of how terrestrial carbon is utilized, altered, and transported within streams. Climate change is expected to influence rainfall patterns and the flow regime of streams (Berghuijs et al., 2014; Botter et al., 2013) and cause shifts in seasonal temperatures—impacting stream metabolism (Ulseth et al., 2018). Our results shed light on the possible consequences of DOM processing and removal within GBs in the face of climate change related shifts in seasonal discharge and temperature. Knowledge of how discharge and temperature affect DOM seasonal and diurnal dynamics in GBs as part of the stream corridor is essential toward improving our current understanding of how reach-scale carbon cycling and the downstream transport of carbon within streams are affected by changing anthropogenic and climatic conditions.

Conflict of Interest

The authors declare that they have no conflict of interest.

Data Availability Statement

Data relating to this publication and analyses conducted can be found online (10.6084/m9.figshare.11358569.v2).

Acknowledgments

This research received funding from the European Union FP7 People: Marie-Curie Actions, Grant/Award 607150. We thank N. Trauth, C. Schmidt, and U. Maier for continued advice and helpful discussion related to the MIN3P model; J. Schelker, G. Steniczka, H. Kraill, S. Schmid, C. Preiler, and M. Mayr for field, laboratory, and other technical assistance; and R. Poeppl and B. Groiss for assistance with topographical surveys and providing equipment.

References

Aitkenhead-Peterson, J. A., McDowell, W. H., & Neff, J. C. (2007). Sources, production, and regulation of allochthonous dissolved organic matter inputs to surface waters. *Aquatic Ecosystems*, 25–70. https://doi.org/10.1016/b978-012256371-3/50003-2

Andersson, C. A., & Bro, R. (2000). The N-way toolbox for MATLAB. *Chemometrics and Intelligent Laboratory Systems*, *52*(1), 1–4. https://doi.org/10.1016/S0169-7439(00)00071-X

Arrigoni, A. S., Poole, G. C., Mertes, L. A. K., O'Daniel, S. J., Woessner, W. W., & Thomas, S. A. (2008). Buffered, lagged, or cooled? Disentangling hyporheic influences on temperature cycles in stream channels. *Water Resources Research*, *44*(9), 1–13. https://doi.org/10.1029/2007WR006480

Bardini, L., Boano, F., Cardenas, M. B., Revelli, R., & Ridolfi, L. (2012). Nutrient cycling in bedform induced hyporheic zones. *Geochimica et Cosmochimica Acta*, *84*, 47–61. https://doi.org/10.1016/j.gca.2012.01.025

Battin, T. J. (1999). Hydrologic flow paths control dissolved organic carbon fluxes and metabolism in an alpine stream hyporheic zone. *Water Resources Research*, *35*(10), 3159–3169. https://doi.org/10.1029/1999WR900144

Battin, T. J. (2000). Hydrodynamics is a major determinant of streambed biofilm activity: From the sediment to the reach scale. *Limnology and Oceanography*, *45*(6), 1308–1319. https://doi.org/10.4319/lo.2000.45.6.1308

Battin, T. J., Kaplan, L. A., Findlay, S., Hopkinson, C. S., Marti, E., Packman, A. I., et al. (2008). Biophysical controls on organic carbon fluxes in fluvial networks. *Nature Geoscience*, *2*(8), 95–100. https://doi.org/10.1038/ngeo602

Battin, T. J., Kaplan, L. A., Newbold, D. J., & Hendricks, S. P. (2003). A mixing model analysis of stream solute dynamics and the contribution of a hyporheic zone to ecosystem function. *Freshwater Biology*, *48*(6), 995–1014. https://doi.org/10.1046/j.1365-2427.2003.01062.x

Battin, T. J., Luyssaert, S., Kaplan, L. A., Aufdenkampe, A. K., Richter, A., & Tranvik, L. J. (2009). The boundless carbon cycle. *Nature Geoscience*, *2*(9), 598–600. https://doi.org/10.1038/ngeo618

Berggren, M., Laudon, H., Jonsson, A., & Jansson, M. (2010). Nutrient constraints on metabolism affect the temperature regulation of aquatic bacterial growth efficiency. *Microbial Ecology*, *60*(4), 894–902. https://doi.org/10.1007/s00248-010-9751-1

Berghuijs, W. R., Woods, R. A., & Hrachowitz, M. (2014). A precipitation shift from snow towards rain leads to a decrease in streamflow. *Nature Climate Change*, *4*. https://doi.org/10.1038/NCLIMATE2246

Boano, F., Harvey, J. W., Marion, A., Packman, A. I., Revelli, R., Ridolfi, L., & Wörman, A. (2014). Hyporheic flow and transport processes: Mechanisms, models, and biogeochemical implications. *Reviews of Geophysics*, *52*(4), 603–679. https://doi.org/10.1002/2012RG000417

Boissier, J. M., Marmonier, P., Claret, C., Fontvieille, D., & Blanc, P. (1996). Comparison of solutes, nutrients, and bacteria inputs from two types of groundwater to the Rhone River during an artificial drought. *Hydrobiologia*, *319*(1), 65–72. https://doi.org/10.1007/BF00020972

Boodoo, K. S., Schmidt, C., Schelker, J., Trauth, N., & Battin, T. J. (2019). Sources and variability of CO_2 in a prealpine stream gravel bar. *Hydrological Processes*, *33*(17), 2279–2299. https://doi.org/10.1002/hyp.13450

Boodoo, K. S., Trauth, N., Schmidt, C., Schelker, J., & Battin, T. J. (2017). Gravel bars are sites of increased CO_2 outgassing in stream corridors. *Scientific Reports*, *7*(1), 14401. https://doi.org/10.1038/s41598-017-14439-0

Botter, G., Basso, S., Rodriguez-Iturbe, I., & Rinaldo, A. (2013). Resilience of river flow regimes. *Proceedings of the National Academy of Sciences*, *110*, 12925–12930. https://doi.org/10.1073/pnas.1311920110

Boulton, A. J., Datry, T., Kasahara, T., Mutz, M., & Stanford, J. A. (2010). Ecology and management of the hyporheic zone: Stream–groundwater interactions of running waters and their floodplains. *Journal of the North American Benthological Society*, *29*(1), 26–40. https://doi.org/10.1899/08-017.1

Briggs, M. A., Lautz, L. K., & Hare, D. K. (2013). Residence time control on hot moments of net nitrate production and uptake in the hyporheic zone. *Hydrological Processes*, *28*(11), 3741–3751. https://doi.org/10.1002/hyp.9921

Casas-Ruiz, J. P., Catalán, N., Gomez-Gener, L., von Schiller, D., Obrador, B., Kothawala, D. N., et al. (2017). A tale of pipes and reactors: Controls on the in-stream dynamics of dissolved organic matter in rivers. *Limnology and Oceanography*, *62*(S1), S85–S94. https://doi.org/10.1002/lno.10471

Coble, P. G. (1996). Characterization of marine and terrestrial DOM in seawater using excitation-emission matrix spectroscopy. *Marine Chemistry*, *51*(4), 325–346. https://doi.org/10.1016/0304-4203(95)00062-3

R Core Team (2017). *R: A language and environment for statistical computing*. Vienna, Austria: R Foundation for Statistical Computing. https://www.R-project.org/

Cory, R. M., & Kaplan, L. A. (2012). Biological lability of streamwater fluorescent dissolved organic matter. *Limnology and Oceanography*, *57*(5), 1347–1360. https://doi.org/10.4319/lo.2012.57.5.1347

Dahm, C. N., Grimm, N. B., Marmonier, P., Vallet, M. H., & Vervier, P. (1998). Nutrient dynamics at the interface between surface waters and groundwaters. *Freshwater Biology*, *40*(3), 427–451. https://doi.org/10.1046/j.1365-2427.1998.00367.x

Duvert, C., Butman, D. E., Marx, A., Ribolzi, O., & Hutley, L. B. (2018). CO_2 evasion along streams driven by groundwater inputs and geomorphic controls. *Nature Geoscience*, *11*(November), 813–818. https://doi.org/10.1038/s41561-018-0245-y

Fasching, C., & Battin, T. J. (2011). Exposure of dissolved organic matter to UV-radiation increases bacterial growth efficiency in a clear-water Alpine stream and its adjacent groundwater. *Aquatic Sciences*, *74*(1), 143–153. https://doi.org/10.1007/s00027-011-0205-8

Fasching, C., Behounek, B., Singer, G. A., & Battin, T. J. (2014). Microbial degradation of terrigenous dissolved organic matter and potential consequences for carbon cycling in brown-water streams. *Scientific Reports*, *4*(1), 1–7. https://doi.org/10.1038/srep04981

Fasching, C., Ulseth, A. J., Schelker, J., Steniczka, G., & Battin, T. J. (2016). Hydrology controls dissolved organic matter export and composition in an Alpine stream and its hyporheic zone. *Limnology and Oceanography*, *61*(2), 558–571. https://doi.org/10.1002/lno.10232

Findlay, S. (1995). Importance of surface-subsurface exchange in stream ecosystems: The hyporheic zone. *Limnology and Oceanography*, *40*(1), 159–164. https://doi.org/10.4319/lo.1995.40.1.0159

Findlay, S., & Sobczak, W. V. (1996). Variability in removal of dissolved organic carbon in hyporheic sediments. *Journal of the North American Benthological Society*, *15*(1), 35–41. https://doi.org/10.2307/1467431

Findlay, S., Strayer, D., Goumbala, C., & Gould, K. (1993). Metabolism of streamwater dissolved organic carbon in the shallow hyporheic zone. *Limnology and Oceanography*, *38*(7), 1493–1499. https://doi.org/10.4319/lo.1993.38.7.1493

Gooseff, M. N., Benson, D. A., Briggs, M. A., Weaver, M., Wollheim, W., Peterson, B., & Hopkinson, C. S. (2011). Residence time distributions in surface transient storage zones in streams: Estimation via signal deconvolution. *Water Resources Research*, *47*(5). https://doi.org/10.1029/2010WR009959

Guillemette, F., & Giorgio, P. A. (2012). Simultaneous consumption and production of fluorescent dissolved organic matter by lake bacterioplankton. *Environmental Microbiology*, *14*(6), 1432–1443. https://doi.org/10.1111/j.1462-2920.2012.02728.x

Hansen, A. M., Kraus, T. E. C., Pellerin, B. A., Fleck, J. A., Downing, B. D., & Bergamaschi, B. A. (2016). Optical properties of dissolved organic matter (DOM): Effects of biological and photolytic degradation. *Limnology and Oceanography*, *61*(3), 1015–1032. https://doi.org/10.1002/lno.10270

Harjung, A., Sabater, F., & Butturini, A. (2018). Hydrological connectivity drives dissolved organic matter processing in an intermittent stream. *Limnologica*, *68*, 71–81. https://doi.org/10.1016/j.limno.2017.02.007

Harvey, J. W., & Fuller, C. C. (1998). Effect of enhanced manganese oxidation in the hyporheic zone on basin-scale geochemical mass balance. *Water Resources Research*, *34*(4), 623–636. https://doi.org/10.1029/97WR03606

Helms, J. R., Stubbins, A., Ritchie, J. D., Minor, E. C., Kieber, D. J., & Mopper, K. (2008). Absorption spectral slopes and slope ratios as indicators of molecular weight, source, and photobleaching of chromophoric dissolved organic matter. *Limonology and Oceanography*, *53*(3), 955–969. https://doi.org/10.4319/lo.2008.53.3.0955

Hendricks, S. P., & White, D. S. (1991). Physicochemical patterns within a hyporheic zone of a northern Michigan River, with comments on surface water patterns. *Canadian Journal of Fisheries and Aquatic Sciences*, *48*(9), 1645–1654. https://doi.org/10.1139/f91-195

Hester, E. T., & Doyle, M. W. (2008). In-stream geomorphic structures as drivers of hyporheic exchange. *Water Resources Research*, *44*(3). https://doi.org/10.1029/2006WR005810

Horgby, Å., Boix Canadell, M., Ulseth, A. J., Vennemann, T. W., & Battin, T. J. (2019). High-resolution spatial sampling identifies groundwater as driver of CO_2 dynamics in an Alpine stream network. *Journal of Geophysical Research, Biogeosciences*, *124*(7), 1961–1976. https://doi.org/10.1029/2019JG005047

Hotchkiss, E. R., Hall, R. O. Jr., Sponseller, R. A., Butman, D., Klaminder, J., Laudon, H., et al. (2015). Sources of and processes controlling CO_2 emissions change with the size of streams and rivers. *Nature Geoscience*, *8*(9), 696–699. https://doi.org/10.1038/ngeo2507

Hudson, N., Baker, A., & Reynolds, D. (2007). Fluorescence analysis of dissolved organic matter in natural, waste and polluted waters—A review. *River Research and Applications*, *649*(April), 631–649. https://doi.org/10.1002/rra

Hunter, W. R., Niederdorfer, R., Gernand, A., Veuger, B., Prommer, J., Mooshammer, M., et al. (2016). Metabolism of mineral-sorbed organic matter and microbial lifestyles in fluvial ecosystems. *Geophysical Research Letters*, *43*(4), 1582–1588. https://doi.org/10.1002/2016GL067719

Inamdar, S., Singh, S., Dutta, S., Levia, D., Mitchell, M., Scott, D., et al. (2011). Fluorescence characteristics and sources of dissolved organic matter for stream water during storm events in a forested mid-Atlantic watershed. *Journal of Geophysical Research, Biogeosciences*, *116*(G3). https://doi.org/10.1029/2011JG001735

Kaplan, L. A., & Bott, T. L. (1982). Diel fluctuations of DOC generated by algae in a piedmont stream. *Limnology and Oceanography*, *27*(6), 1091–1100. https://doi.org/10.4319/lo.1982.27.6.1091

Kaplan, L. A., & Bott, T. L. (1989). Diel fluctuations in bacterial activity on streambed substrata during vernal algal blooms: Effects of temperature, water chemistry, and habitat. *Limnology and Oceanography*, *34*(4), 718–733. https://doi.org/10.4319/lo.1989.34.4.0718

Kaplan, L. A., Wiegner, T. N., Newbold, J. D., Ostrom, P. H., & Gandhi, H. (2008). Untangling the complex issue of dissolved organic carbon uptake: A stable isotope approach. *Freshwater Biology*, *53*(5), 855–864. https://doi.org/10.1111/j.1365-2427.2007.01941.x

Kasahara, T., & Wondzell, S. M. (2003). Geomorphic controls on hyporheic exchange flow in mountain streams. *Water Resources Research*, *39*(1), SBH 3-1–SBH 3-14. https://doi.org/10.1029/2002WR001386

Kragh, T., Søndergaard, M., & Tranvik, L. (2008). Effect of exposure to sunlight and phosphorus-limitation on bacterial degradation of coloured dissolved organic matter (CDOM) in freshwater. *FEMS Microbiology Ecology*, *64*(2), 230–239. https://doi.org/10.1111/j.1574-6941.2008.00449.x

Leichtfried, M. (1988). Bacterial substrates in gravel beds of a second order alpine stream (Project Ritrodat-Lunz, Austria). *SIL Proceedings, 1922-2010*, *23*, 1325–1332. https://doi.org/10.1080/03680770.1987.11898016

Marmonier, P., Fontvieille, D., Gibert, J., & Vanek, V. (1995). Distribution of dissolved organic carbon and bacteria at the interface between the Rhône River and its alluvial aquifer. *Journal of the North American Benthological Society*, *14*(3), 382–392. https://doi.org/10.2307/1467204

McKnight, D. M., Boyer, E. W., Westerhoff, P. K., Doran, P. T., Kulbe, T., & Anderson, D. T. (2001). Spectroflourometric characterization of dissolved organic matter for indication of precursor organic material and aromaticity. *Limnology and Oceanography*, *46*(1), 38–48. https://doi.org/10.4319/lo.2001.46.1.0038

Mulholland, P. J., Marzolf, E. R., Webster, J. R., Hart, D. R., Hendricks, S. P., & Station, H. B. (1997). Evidence that hyporheic zones increase heterotrophic metabolism and phosphorus uptake in forest streams. *42*(3), 443–451. https://doi.org/10.4319/lo.1997.42.3.0443

Parlanti, E., Woerz, K., Geoffroy, M., & Lamotte, M. (2000). Dissolved organic matter fluorescence spectroscopy as a tool to estimate biological activity in a coastal zone submitted to anthropogenic inputs. *Organic Geochemistry*, *31*(12), 1765–1781. https://doi.org/10.1016/S0146-6380(00)00124-8

Raymond, P. A., Hartmann, J., Lauerwald, R., Sobek, S., Mcdonald, C., Hoover, M., et al. (2013). Global carbon dioxide emissions from inland waters. *Nature*, *503*(7476), 355–359. https://doi.org/10.1038/nature12760

Raymond, P. A., & Spencer, R. G. M. (2015). Riverine DOM. In *Biochemistry of Marine Dissolved Organic Matter* (pp. 509–533). Academic Press.

Schindler, J. E., & Krabbenhoft, D. P. (1998). The hyporheic zone as a source of dissolved organic carbon and carbon gases to a temperate forested stream. *Biogeochemistry*, *43*(2), 157–174. https://doi.org/10.1023/A:1006005311257

Schmidt, M. W. I., Torn, M. S., Abiven, S., Dittmar, T., Guggenberger, G., Janssens, I. A., et al. (2011). Persistence of soil organic matter as an ecosystem property. *Nature*, *478*(7367), 49–56. https://doi.org/10.1038/nature10386

Singh, S., Inamdar, S., Mitchell, M., & Mchale, P. (2014). Seasonal pattern of dissolved organic matter (DOM) in watershed sources: Influence of hydrologic flow paths and autumn leaf fall. *Biogeochemistry*, *118*(1-3), 321–337. https://doi.org/10.1007/s10533-013-9934-1

Sokol, R. R., & Rohlf, F. J. (1969). *The principles and practice of statistics in biological research*. San Francisco, CA: Freeman.

Spencer, R. G. M., Pellerin, B. A., Bergamaschi, B. A., Downing, B. D., Kraus, T. E. C., Smart, D. R., et al. (2007). Diurnal variability in riverine dissolved organic matter composition determined by in situ optical measurement in the San Joaquin River (California, USA). *Hydrological Processes*, *21*, 3181–3189. https://doi.org/10.1002/hyp

Stedmon, C. a., & Bro, R. (2008). Characterizing dissolved organic matter fluorescence with parallel factor analysis: A tutorial. *Limnology and Oceanography: Methods*, *6*(11), 572–579. https://doi.org/10.4319/lom.2008.6.572

Stedmon, C. A., & Markager, S. (2005). Tracing the production and degradation of autochthonous fractions of dissolved organic matter by fluorescence analysis. *Limnology and Oceanography*, *50*(5), 1415–1426.

Stegen, J. C., Fredrickson, J. K., Wilkins, M. J., Konopka, A. E., Nelson, W. C., Arntzen, E. V., et al. (2016). Groundwater-surface water mixing shifts ecological assembly processes and stimulates organic carbon turnover. *Nature Communications*, *7*(1), 1, 11237–12. https://doi.org/10.1038/ncomms11237

Stonedahl, S. H., Harvey, J. W., Wörman, A., Salehin, M., & Packman, A. I. (2010). A multiscale model for integrating hyporheic exchange from ripples to meanders. *Water Resources Research*, *46*(12), 1–14. https://doi.org/10.1029/2009WR008865

Tonina, D., & Buffington, J. M. (2007). Hyporheic exchange in gravel bed rivers with pool-riffle morphology: Laboratory experiments and three-dimensional modeling. *Water Resources Research*, *43*(1), 1–16. https://doi.org/10.1029/2005WR004328

Tonina, D., & Buffington, J. M. (2009). Hyporheic exchange in mountain rivers I: Mechanics and environmental effects. *Geography Compass*, *3*(3), 1063–1086. https://doi.org/10.1111/j.1749-8198.2009.00226.x

Tonina, D., & Buffington, J. M. (2011). Effects of stream discharge, alluvial depth and bar amplitude on hyporheic flow in pool-riffle channels. *Water Resources Research*, *47*(8), 1–13. https://doi.org/10.1029/2010WR009140

Tranvik, L. J., & Bertilsson, S. (2001). Contrasting effects of solar UV radiation on dissolved organic sources for bacterial growth. *Ecology Letters*, *4*(5), 458–463. https://doi.org/10.1046/j.1461-0248.2001.00245.x

Trauth, N., Schmidt, C., Maier, U., & Fleckenstein, J. H. (2014). Influence of varying hydraulic conditions on hyporheic exchange and reactions in an in-stream gravel bar, 16, 14,317

Trulleyová, Š., Rulík, M., & Popelka, J. (2003). Stream and interstitial water DOC of a gravel bar (Sitka stream, Czech Republic): Characteristics, dynamics and presumable origin. *Archiv für Hydrobiologie*, *158*(3), 407–420. https://doi.org/10.1127/0003-9136/2003/0158-0407

Ulseth, A. J., Bertuzzo, E., Singer, G. A., Schelker, J., & Battin, T. J. (2018). Climate-induced changes in spring snowmelt impact ecosystem metabolism and carbon fluxes in an Alpine stream network. *Ecosystems*, *21*(2), 373–390. https://doi.org/10.1007/s10021-017-0155-7

Vervier, P., Dobson, M., & Pinay, G. (1993). Role of interaction zones between surface and ground waters in DOC transport and processing: Considerations for river restoration. *Freshwater Biology*, *29*(2), 275–284. https://doi.org/10.1111/j.1365-2427.1993.tb00763.x

Weishaar, J., Aiken, G., Bergamaschi, B., Fram, M., Fujii, R., & Mopper, K. (2003). Evaluation of specific ultra-violet absorbance as an indicator of the chemical content of dissolved organic carbon. *Environmental Science and Technology*, *37*(20), 4702–4708. https://doi.org/10.1021/es030360x

Wong, J. C. Y., & Williams, D. D. (2010). Sources and seasonal patterns of dissolved organic matter (DOM) in the hyporheic zone. *Hydrobiologia*, *647*(1), 99–111. https://doi.org/10.1007/s10750-009-9950-2

Wu, L., Singh, T., Gomez-velez, J., Gunnar, N., Anders, W., & Krause, S. (2018). Impact of dynamically changing discharge on hyporheic exchange processes under gaining and losing groundwater conditions. *Water Resources Research*, *54*(12). https://doi.org/10.1029/2018WR023185

Yvon-Durocher, G., Caffrey, J. M., Cescatti, A., Dossena, M., Del Giorgio, P., Gasol, J. M., et al. (2012). Reconciling the temperature dependence of respiration across timescales and ecosystem types. *Nature*, *487*(7408), 472–476. https://doi.org/10.1038/nature11205

Zsolnay, A., Baigar, E., Jimenez, M., Steinweg, B., & Saccomandi, F. (1999). Differentiating with fluorescence spectroscopy the sources of dissolved organic matter in soils subjected to drying. *Chemosphere*, *38*(1), 45–50. https://doi.org/10.1016/S0045-6535(98)00166-0